Nucleic Acids Research, 1996, Vol. 24, No. 10 **1901–1907**

Potent antisense oligonucleotides to the human multidrug resistance-1 mRNA are rationally selected by mapping RNA-accessible sites with oligonucleotide libraries

Siew Peng Ho*, Dustin H. O. Britton, Barry A. Stone, Davette L. Behrens, Lynn M. Leffet, Frank W. Hobbs, Jeff A. Miller and George L. Trainor

DuPont Merck Research Laboratories, PO Box 80400 Experimental Station, Wilmington, DE 19880-0400, USA

Received January 19, 1996; Revised and Accepted March 27, 1996

ABSTRACT

Antisense oligonucleotides can vary significantly and unpredictably in their ability to inhibit protein synthesis. Libraries of chimeric oligonucleotides and RNase H were used to cleave and thereby locate sites on human multidrug resistance-1 RNA transcripts that are relatively accessible to oligonucleotide hybridization. In cell culture, antisense sequences designed to target these sites were significantly more active than oligonucleotides selected at random. This methodology should be generally useful for identification of potent antisense sequences. Correlation between oligonucleotide activity in the cell culture assay and in an *in vitro* RNase H assay supports the proposed role of the enzyme in the mechanism of antisense suppression in the cell.

INTRODUCTION

The use of antisense DNA oligonucleotides (ODNs) for inhibition of protein synthesis is well established and fairly widespread (1–3). In addition to their use as research tools, antisense ODNs are currently being evaluated in several clinical trials as potential therapeutic agents. However, as numerous examples demonstrate (4–6), the factors which influence the potency of antisense sequences are complex and poorly understood; consequently the selection of such sequences has largely been empirical. Since the mRNA target of antisense inhibition is folded into secondary and tertiary structures, some sites that might otherwise be available for hybridization with ODNs may be rendered inaccessible. The regions of an mRNA that are commonly targeted include the 5′-untranslated region, the 3′-untranslated region, splice sites and the region around the translation initiation codon (AUG). Of these sites, targeting an ODN to the AUG region has most consistently demonstrated an antisense effect, nevertheless, the AUG site is by no means the only region that produces an antisense effect nor is it the region that necessarily produces the most potent effect. Additionally, because nucleotide sequences around the AUG (and around splice sites) are somewhat conserved (7), other mRNA targets may be inadvertently affected by antisense sequences designed to those regions. Design strategies that take into account the G,C content or duplex melting temperatures (T_m) (4) and RNA folding programs (8,9) have also produced mixed results.

A method was therefore devised for locating sites on an mRNA molecule that are most accessible to hybridization with antisense ODNs. This was accomplished (Fig. 1a) by probing an RNA transcript with a library of chemically synthesized, semi-random ODNs. When mixed together, the accessible regions of the RNA should hybridize with complementary sequences found within the library. These regions are subsequently identified using RNase H, which catalyzes the hydrolytic cleavage of the phosphodiester backbone of only the RNA strand of a hybrid RNA–DNA duplex. Sequencing of the RNA fragments produced should allow identification of those regions in a particular mRNA sequence which can serve as sites for targeting ODNs. Since the mechanism of antisense inhibition is believed to frequently involve RNase H, the use of RNase H/ODN libraries for the mapping of accessible sites is likely to be more relevant than approaches involving either other ribonucleases (10,11) or chemical agents (12,13).

MATERIALS AND METHODS

Synthesis of oligonucleotide libraries

Libraries and phosphorothioate ODNs were chemically synthesized using an automated RNA/DNA ABI 394 synthesizer (Applied Biosystems). For the libraries, all nucleotide positions with the exception of the constrained nucleotide were synthesized using a mixture of phosphoramidites in a ratio of 1.5:1.25:1.15:1.0 (A:C:G:U/T), believed to produce a random mixture of sequences. Sulfurization of ODNs was accomplished using the Beaucage reagent (Glen Research). ODNs were purified by reverse phase HPLC (PRP-3 column; Hamilton Co.) and analyzed by capillary gel electrophoresis (P/ACE 2100; Beckman).

In vitro transcription

RNA was transcribed from the pMDR2000xs.Seq plasmid (the plasmid was a generous gift from Dr Michael Gottesman) which

* To whom correspondence should be addressed

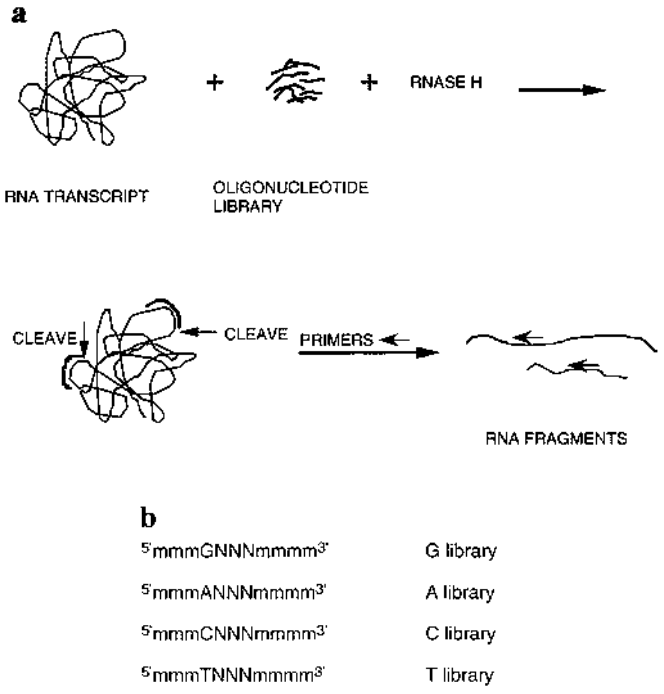

Figure 1. (**a**) Scheme for antisense sequence selection. A library of chimeric ODNs is allowed to hybridize with an RNA molecule. The RNA in the DNA–RNA duplex is cleaved with RNase H. The resulting fragments are gel and sequence analyzed to locate the accessible sites and the information obtained is used to design antisense sequences. (**b**) Sequence of the chimeric ODN libraries. G, A, C and T are deoxyribonucleotides. m and N denote a random mixture of 2′-methoxyribonucleotide and deoxyribonucleotide bases respectively.

encodes the full-length P-glycoprotein. The plasmid was linearized with *Sca*I and then transcribed with T7 RNA polymerase using the RiboMAX kit (750 nmol rNTPs, 500 nmol guanosine, total volume 100 µl; Promega). The RNA was extracted with phenol/chloroform/isoamyl alcohol, passed through a G-50 Sephadex Quick Spin column (Boehringer Mannheim), ethanol precipitated and 5′-end-labeled under standard conditions with T4 polynucleotide kinase.

Mapping and *in vitro* RNase H experiments

Libraries and ODNs were treated with proteinase K (12 µg/µl for 3 h at 37°C) prior to use. They were extracted (phenol/chloroform/isoamyl alcohol), ethanol precipitated, resuspended in diethylpyrocarbonate-treated water and quantitated by UV spectrometry. Assays was run in sterile 96-well microtiter dishes (GeNunc Modules). In mapping experiments, 10 nM 5′-^{32}P-labeled RNA transcript was incubated separately with each semi-random library (30 µM) and 0.1 U/µl RNase H (Promega) at 37°C for 20 min in a Tris buffer (40 mM Tris, pH 8.0, 4 mM $MgCl_2$, 1 mM DTT, 10 µl total volume). The reactions were quenched with formamide gel loading buffer and the samples loaded on a 6% denaturing polyacrylamide gel. Gels were analyzed with a PhosphorImager (Molecular Dynamics). (Data shown represent a linear relationship between signal and image intensity.) In *in vitro* RNase H experiments using individual ODNs, 200 nM phosphorothioate ODNs were incubated with transcript and enzyme; all other conditions were identical.

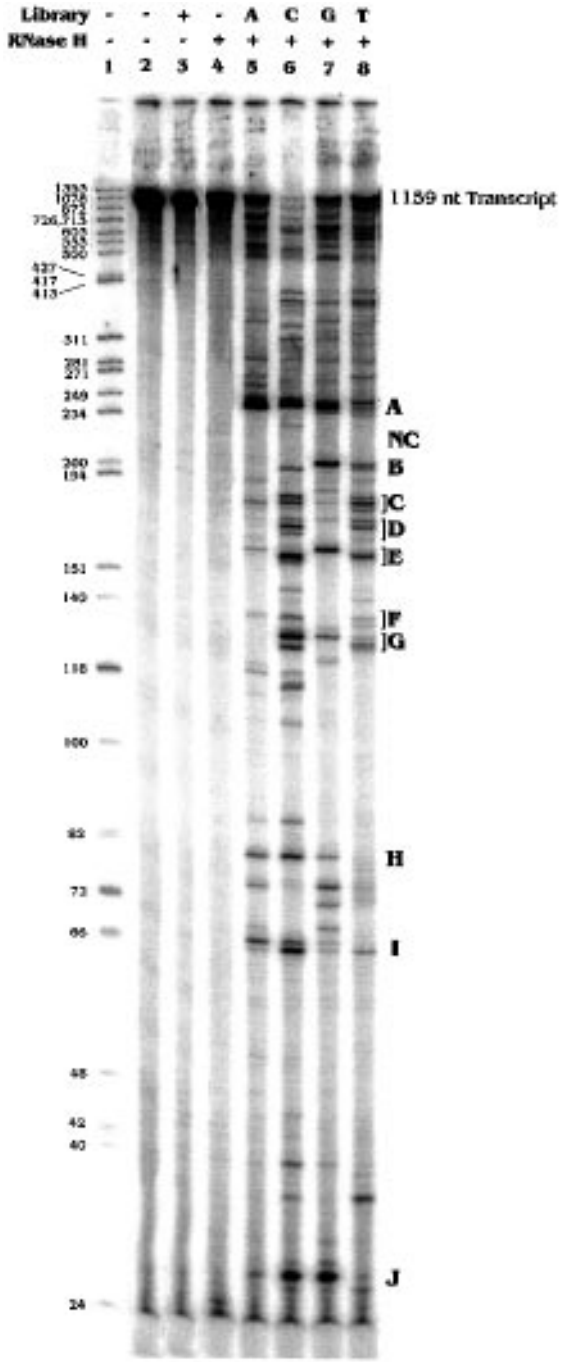

Figure 2. Autoradiogram of RNA fragments showing cleavage at accessible sites. Lane 1, DNA markers; lane 2, 5′-end-labeled transcript; lane 3, RNA together with all four chimeric libraries; lane 4, RNA together with RNase H; lanes 5–8, RNA incubated with individual libraries and RNase H. RNA fragments corresponding to accessible sites are labeled A–J.

Primer extension analysis

A large scale RNase H assay (equivalent to 20 microtiter wells) was performed with unlabeled transcript. The reaction mixture was then extracted, ethanol precipitated and filtered through a Quick Spin column (Rainin). The recovered mixture of full-

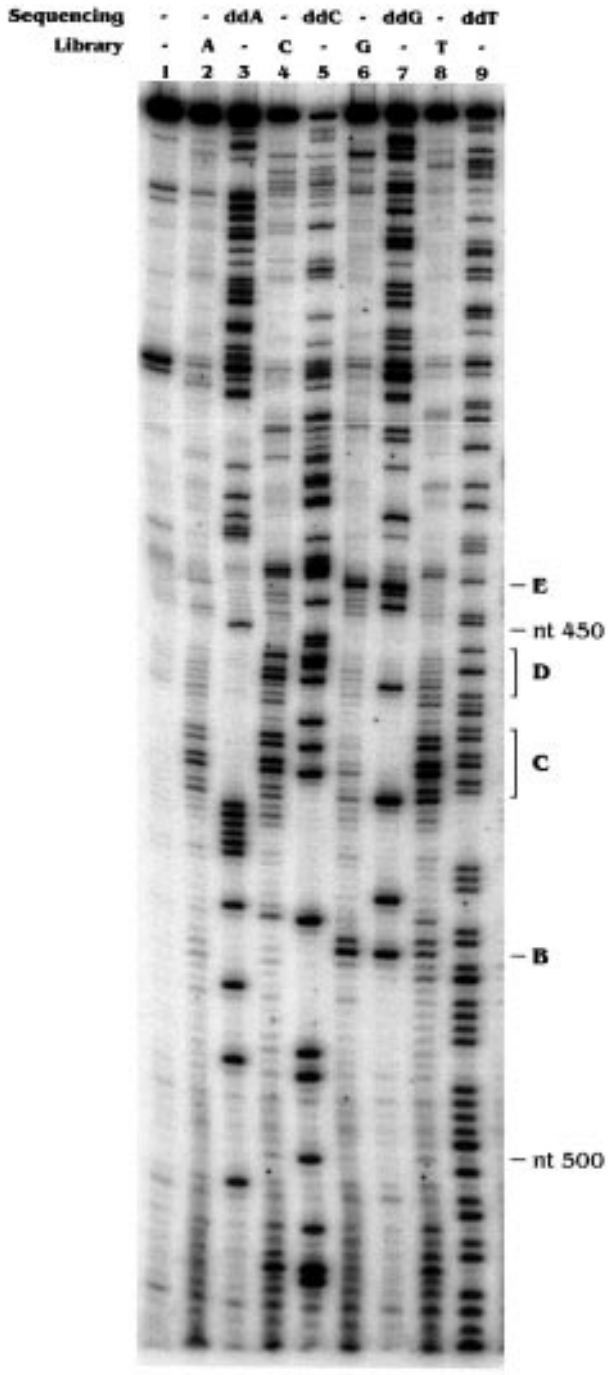

Figure 3. Autoradiogram identifying the location of sites B–E through primer extension analysis. The primer was designed to hybridize to nt 518–537 (Fig. 4) of the RNA. Control lane 1, primer extension of the full-length transcript. Sequencing lanes 3, 5, 7 and 9, primer extension of the full-length transcript in the presence of ddT, ddG, ddC and ddA respectively. Lanes 2, 4, 6 and 8, primer extension of RNA fragments generated by treatment of full-length transcript with the libraries and RNase H. The numbering system is based on Figure 4.

length and cleaved transcript was used as the template for primer extension analysis (42°C for 30 min) with several different 5′-^{32}P-labeled primers (150 nM) and AMV reverse transcriptase (1.2 U/μl; Promega). Primer extension of the full-length transcript with dNTPs served as the control. RNA sequencing lanes (from primer extension of full-length transcript with ddNTPs) were interspersed with primer extension lanes (with dNTPs) of the cleaved fragments.

Cell culture experiments

The cell-based assay was adapted from a method by Trevorrow (14). Human MDR-positive epithelial carcinoma cells (KB8-5) were incubated with a complex of ODN and lipofectin (Gibco-BRL) (final concentrations 1 and 7 μM respectively) in serum-free medium for 3 days (37°C, 5% CO_2). The cells were scraped and incubated, first with rhodamine-123 (2.5 μg/ml, 55 min) and then with propidium iodide (5 μg/ml, 5 min). After washing, verapamil (40 μM) was added to the positive control cells; all samples were then incubated for 1 h. After gating out dead cells, the mean intracellular concentration of rhodamine in 10 000 cells was determined by flow cytometry (Becton Dickinson FAC-Scan). The mean rhodamine signal in ODN-treated cells was scaled relative to verapamil-treated cells. Cells that received neither ODN nor verapamil served as negative controls.

RESULTS AND DISCUSSION

The semi-random libraries used consist of 11 nt oligomers. Ten of the 11 nucleotide positions were synthesized to contain a random mixture of bases. The identity of the eleventh nucleotide at an internal position was constrained, as experiments with the completely random library gave far less optimal results. However, to ensure the sampling of every possible sequence, all four libraries with a single constrained nucleotide were synthesized and tested (Fig. 1b). The libraries are chimeric ODNs composed of a mixture of deoxyribonucleotides with 2′-methoxyribonucleotide flanks. Incorporation of 2′-methoxyribonucleotides increases the thermodynamic stability of the 11 nt duplex between ODN and RNA (15,16). Additionally, such chimeric ODNs selectively direct RNase H cleavage to primarily one position per duplex, as opposed to multiple positions when mediated by an all-phosphodiester ODN (17,18).

This methodology was applied to a 1159 nt transcript of the h*MDR1* gene. In the absence of enzyme (Fig. 2, lane 3) or library (lane 4) the transcript remained intact. However, when all three components were present together, discrete cleavage fragments of varying intensity were obtained (lanes 5–8). As the activity of RNase H is not sequence dependent (19,20), these results support the hypothesis that not all regions of an RNA molecule are equally accessible for hybridization with ODNs. Furthermore, the cleavage patterns vary depending on the identity of the constrained nucleotide in the library. Since these ODNs are only 11 bases long and since the constrained nucleotide is at an internal position, a mismatch with that constrained nucleotide may be sufficient to destabilize and hence disrupt any partially hybridized duplex. Therefore, not all libraries will identify the same accessible sites. A total of 10 accessible sites (Fig. 2), A–J, were identified in the first 250 nt of the transcript. Experiments with a completely random library produced cleavage patterns that were far less intense; this may be due to the greater likelihood of self-hybridization occuring amongst members of the library. Although these experiments were carried out on a 1159 nt transcript, experiments with other h*MDR1* transcripts (800 and 3000 nt) demonstrate that the same sites are identified provided the same 5′-end is retained. Location of these sites was identified

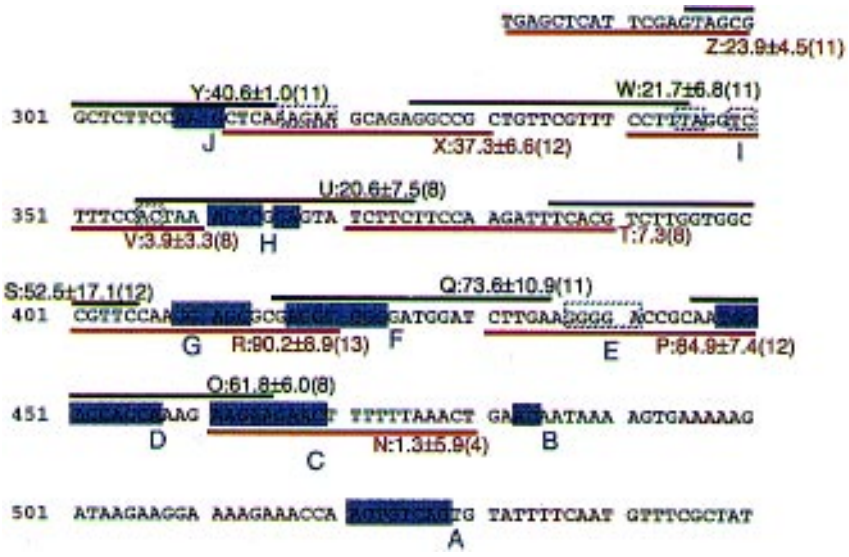

Figure 4. Inhibition of P-glycoprotein function of ODNs selected by walking the RNA. Accessible sites identified by mapping are boxed or outlined in blue. Mapping ODNs were not made to sites E and I (hatched boxes). The regions targeted by walking ODNs (N–Z) are represented by either the red or green bars. Following the ODN name is the percent antisense inhibition by that ODN (relative to verapamil), followed by the number of G and C residues in the sequence in parenthesis. The average inhibition produced by a generic negative control ODN $(N)_{19}T$ was 7.1 ± 5.6%.

by reverse transcriptase-mediated primer extension of the 3′-fragments (Fig. 3). Primer extension of the full-length transcript (lane 1) is an important control, ensuring that sites identified in the even numbered lanes are genuine accessible sites, as opposed to bands arising from primer termination due to RNA secondary structure. As with the mapping results of Figure 2, the primer extension data also shows that not all libraries identify the same sites. Additionally, within any one site, the cleavage fragments generated are of varying intensity.

The data obtained above was used in the selection of 20 nt phosphorothioate ODNs (called the mapping ODNs), designed to hybridize at eight of the accessible sites identified. Two negative control ODNs (NC1 and NC2) were selected to hybridize to the region between sites A and B. The accessible sites identified are summarized either as a range of nucleotides (Table 1) or as boxed regions (Fig. 4). Since chimeric ODNs in the 11mer library mediate cleavage of the RNA strand only in regions base paired with deoxyribonucleotides (17,18), any chimeric ODN should hybridize to the RNA with its 5′-end extending at least 3 nt beyond the cleaved base. Therefore, a series of phosphorothioate ODNs (e.g. A1, A2 and A3 to site A) was designed to each site such that the 5′-end of the ODN extends beyond individual cleaved bases to different degrees.

The ability of these ODNs to inhibit the synthesis of P-glycoprotein (the protein encoded by the h*MDR1* gene) was tested in KB8-5 cells. Due to low P-glycoprotein expression in these cells, we and others have not been able to reliably quantitate P-glycoprotein levels (21). However, the correlation between increased P-glycoprotein expression and the multidrug resistance phenotype (indiscriminate efflux of a wide range of hydrophobic, cytotoxic compounds) is well documented (22). Furthermore, the use of the rhodamine efflux assay as an indicator of P-glycoprotein expression and function has been validated (23,24). Therefore, the efficacy of antisense ODNs in the inhibition of P-glycoprotein function was determined using the rhodamine assay. After treatment with antisense ODNs, the cells were incubated with rhodamine. Functional P-glycoprotein actively pumps rhodamine out of the cells. Intracellular rhodamine concentrations determined by fluorescence activated cell sorting (FACS) provided a readout of P-glycoprotein function. Experiments in the presence and absence of verapamil, a competitive inhibitor of P-glycoprotein, were used as positive and negative controls respectively and served to demarcate the range of inhibition possible. However, since inhibition by verapamil occurs by a different mechanism from that of antisense ODNs, it is possible for ODN inhibition to fall outside the range defined by verapamil. A 15 nt phosphorothioate ODN previously described in the literature (5) produced a 68% inhibition of P-glycoprotein function in this assay. Four negative controls, a 2 base and a 4 base mismatch to the antisense sequence, a scrambled sequence as well as a generic negative control $(N)_{14}T$, run alongside the antisense ODN all inhibited P-glycoprotein function to <10% (G.L.Trainor *et al.*, manuscript in preparation). The generic control consists of randomized bases at all positions except for the terminal 3′ nucleotide.

Mapping ODNs were therefore tested in the rhodamine assay using a similar randomized sequence $(N)_{19}T$ as a generic control. The data (Table 1) shows that both negative control sequences complementary to the region between sites A and B exhibited no significant antisense effects. However, ODNs complementary to accessible sites exhibited a range of activity. Oligonucleotides to three sites (D, F and G) showed a strong inhibitory effect on P-glycoprotein function (>80% inhibition relative to verapamil). Oligonucleotides to site J were moderately active, while those to the remaining sites (A–C and H) produced poor antisense inhibition. Within each site, moving the 5′-end of the ODN by 2–3 nt could affect the antisense activity by as much as 20–30%.

Table 1. Inhibition of P-glycoprotein function by mapping ODNs designed against accessible sites

Site (location)	Oligonucleotide name	Oligonucleotide location	Percent antisense inhibition	No. of G,C bases
A (521–528)	A1	508–527	14.9 ± 2.9	8
	A2	510–529	16.0 ± 3.4	7
	A3	512–531	35.1 ± 2.8[a]	8
B (483–484)	B1	471–490	7.5 ± 1.7	3
	B2	474–493	2.5 ± 1.4	4
C (461–469)	C1	445–464	33.5 ± 14.3	9
	C2	448–467	30.5 ± 7.1	9
	C3	451–470	7.7 ± 4.2[a]	8
D (448–457)	D1	432–451	79.5 ± 7.0	11
	D2	435–454	112.1 ± 13.1	12
	D3	438–457	91.1 ± 3.9	13
F (417–423)	F1	402–421	83.5 ± 6.5[a]	13
	F2	404–423	85.1 ± 0.1[a]	14
	F3	407–426	114.1 ± 2.5[a]	13
G (409–413)	G1	394–413	82.9 ± 22.5[a]	13
	G2	396–415	85.9 ± 2.1[a]	14
H (361–364)	H1	348–367	9.6 ± 2.0	9
	H2	351–370	15.7 ± 2.2	8
J (309–311)	J1	294–313	46.2 ± 5.9[a]	11
	J2	296–315	45.6 ± 5.6[a]	11
NC	NC1	498–517	3.6 ± 2.1[a]	5
	NC2	484–503	–0.72 ± 2.4	4

Antisense ODNs were designed to eight accessible sites including a negative control region (NC). The nt numbering system is that of the hMDR1.GB_PR gene sequence (25; accession no. M14758), with the translation and major transcription initiation sites at positions 425 and 285 respectively (see also Fig. 4).
[a]Two-point data sets; the remaining ODNs were tested at least three times. The average inhibition produced by a generic, 20 nt negative control oligonucleotide having a random sequence $(N)_{19}T$ was 10.2 ± 4.6%.

When these results were analyzed in the context of G,C content of the ODNs, a correlation was observed (Table 1). Oligonucleotides with a minimum of 11 G or C residues exhibited moderate to strong inhibition, while ODNs having nine or less G and C residues had poor antisense activity. Although duplex melting temperatures and G,C content are generally not accurate predictors of antisense ODN efficacy (4), we hypothesized that the absence of significant antisense effects at accessible sites A–C and H may indeed be linked to poor duplex stability of the phosphorothioate ODN–RNA duplex. If the melting temperatures of these A,T-rich ODNs could be increased, a significant antisense effect might be observed. To evaluate this hypothesis, we prepared several chimeric ODNs similar in structure to those ODNs used in the libraries. These chimeras contain six 2′-methoxyribonucleotide bases at each end of the ODN but differ from the libraries by having phosphorothioate lingkages. Chimeras were made of a negative control ODN (NC2), an ODN with potent activity (D2) and two ODNs having nine G and C residues but with little antisense activity (C2 and H1). The results (Table 2) show that while the chimeric analog of D2 (CD2) retains its potent antisense activity, the homolog of NC2 (CNC2) remains inactive. In contrast, the chimeric versions of two ODNs targeted to sites shown by mapping to be accessible exhibited significant increases in potency. Oligonucleotide CC2, which is identical in sequence to ODN C2, had an 80% increase in antisense activity; similarly ODN CH1 had a 110% increase over ODN H1. These results suggest that the lack of activity previously observed at these A,T-rich sites with phosphorothioate ODNs was likely due to the lack of thermodynamic stability of the ODN–RNA duplexes.

Our mapping data indicates that the first 200 nt of the h*MDR1* transcript has a high density of accessible sites and therefore appears to be particularly susceptible to antisense inhibition. Prior to the mapping studies, a set of 13 ODNs (walking ODNs) had been chosen by systematically walking the first 200 nt of the h*MDR1* message. These ODNs span the region containing sites C–J. Each 20 nt phosphorothioate ODN overlaps the next member of the series by 5 nt (Fig. 4). To further evaluate the mapping methodology, ODNs selected by this alternate method were compared with ODNs selected through the mapping method. As expected, there was a wide range in the ability of these walking ODNs to elicit an antisense effect in cell culture. Of the 13 ODNs, three had potent antisense effects (>70% with respect to verapamil), three were modest in their activity (40–70%) and the rest were poor. Unlike the mapping ODNs, there was no correlation between efficacy and number of G or C residues present. For instance, ODNs W and Z (Fig. 4), which have 11 G and C residues, both have low levels of antisense activity. Rather, potency of these walking ODNs tracked better with proximity to accessible sites. For example, the 5′-end of ODN P is proximal to site D, while the 5′-end of ODN R is in the vicinity of site F. (RNase H cleaves the RNA of a hybrid duplex in the vicinity of the 5′-end of DNA ODNs.) Likewise, sequences such as ODN U and ODN T, whose 5′-ends are not in the vicinity of identified accessible regions, were found to have little antisense activity. Our data therefore suggests that, in general, a high G,C content by itself is insufficient to produce a potent antisense effect if an inaccessible region is targeted. This is consistent with previous reports that a high duplex melting temperature between an ODN and its RNA target does not necessarily translate into potent inhibitory antisense effects in cell culture (4).

Table 2. Chimeric ODNs have potent antisense effects when targeted to accessible sites that are A,T-rich

Experiment	Thioate oligonucleotide	Percent antisense inhibition	Chimeric oligonucleotide	Percent antisense inhibition
1	NC2	1.7	CNC2	8.3
2	NC2	–3.2	CNC2	7.5
1	D2	130.9	CD2	146.7
2	D2	127.0	CD2	140.8
1	C2	23.0	CC2	92.7
2	C2	24.8	CC2	114.7
1	H1	9.3	CH1	126.1
2	H1	10.6	CH1	113.5

Results of two separate experiments where side-by-side comparisons between phosphorothioate versus chimeric ODNs were made. The average inhibition produced by the generic negative control ODN $(N)_{19}T$ was 13.6 ± 6.8%. The chimeric version of the generic negative control ODN produced an inhibition of 7.5 ± 2.5%.

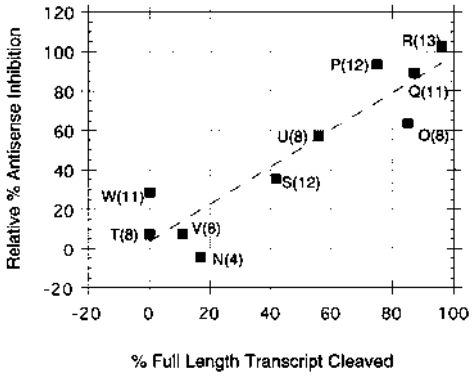

Figure 5. Correlation of ODN activity in cell culture and in an *in vitro* assay. The inhibition of P-glycoprotein function by 10 of the randomly selected walking ODNs (N–W, all examined in the same experiment) was plotted against the amount of transcript cleaved by RNase H in the presence of that ODN. Each ODN (200 nM) was reacted with transcript (10 nM) and RNase H (0.1 U/µl) for 20 min. The number of G and C residues in each sequence is shown in parenthesis.

Both mapping and walking ODNs were also examined in an *in vitro* RNase H assay. In these experiments, individual ODNs were incubated with transcript in the presence of RNase H. The amount of RNA cleavage mediated by any one ODN was then quantitated and the data compared with results obtained from cell culture. A strong correlation ($r = 0.92$) was obtained between the *in vitro* and cell culture data (Fig. 5) for the walking ODNs; a similar though less strong correlation was obtained with the mapping ODNs. These data suggest that an *in vitro* RNase H assay can serve as an accurate predictor of ODN efficacy in cell culture. Furthermore, the data suggests the participation of RNase H in the mechanism of antisense suppression.

To summarize, eight major accessible sites (C–J) were identified in the first 200 nt of the h*MDR1* transcript. Of these, mapping ODNs were designed to six of the sites to determine the usefulness of RNA mapping experiments for antisense sequence selection. Phosphorothioate or chimeric ODNs designed to these sites were highly active (>80% activity) in the cell-based assay in five of the six cases. (If ODNs had been designed to site E, it is likely that their activity would have exceeded 80%, based on the activity of ODN Q; Fig. 4.) In comparison, when this same region of the RNA was surveyed with ODNs (walking) spaced at regular intervals, three of the 13 sequences examined showed antisense activity >70%. The high density of accessible sites in this portion of the h*MDR1* transcript increased the likelihood of identifying active sequences by walking the RNA. The three most potent walking ODNs are proximal to accessible sites. Additionally, even though these sequences (ODNs P, R and Q) were coincidentally well placed with respect to accessible sites, they were by no means optimally placed for maximum antisense efficacy. For instance, at sites D and F, mapping ODNs D2 and F3 were more potent than walking ODNs P and R by 21 and 28% respectively when assayed side-by-side in the same experiment (data not shown). Lastly, of the nine mapping sequences that produce antisense effects >80%, only two ODNs (F2 and F3) are in the 6 nt 'consensus region' around the AUG. Since this mapping strategy can identify active antisense sequences throughout the entire length of the transcript, the unintentional targeting of other RNA molecules (currently known or as yet unsequenced) can be potentially minimized.

Antisense activity of any ODN appears to depend on the accessibility of its target site. Methodology has been developed using RNase H and chimeric ODN libraries which allows identification of such sites. This methodology may be particularly useful with high molecular weight mRNA species such as from the h*MDR1* gene, where alternative approaches such as systematic 'walking' of the entire RNA and screening of multiple antisense sequences becomes impractical. Once the accessibility requirement is satisfied, antisense ODNs must have a minimum G,C content to demonstrate an adequate antisense response. A,T-rich phosphorothioate ODNs may not hybridize to their target RNA sites with sufficient thermodynamic stability to allow efficient processing by RNase H. Such regions can, however be successfully targeted with T_m-enhancing analogs such as chimeras containing 2′-methoxyribonucleotides.

REFERENCES

1 Crooke,S.T. and Lebleu,B. (1993) *Antisense Research and Applications.* CRC Press, Boca Raton, FL.
2 Akhtar,S. (1995) In Akhtar,S. (Ed.), *Delivery Strategies for Antisense Oligonucleotide Therapeutics.* CRC Press, Boca Raton, FL.
3 Wagner,R.W. (1994) *Nature*, **372**, 333–335.
4 Chiang,M.-Y., Chan,H., Zounes,M.A., Freier,S.M., Lima,W.F. and Bennett,C.F. (1991) *J. Biol. Chem.*, **266**, 18162–18171.
5 Jaroszewski,J.W., Kaplan,O., Syi,J.-L., Sehested,M., Faustino,P.J. and Cohen,J.S. (1990) *Cancer Commun.*, **2**, 287–294.
6 Peyman,A., Helsberg,M., Kretzschmar,G., Mag,M., Gravley,S. and Uhlmann,E. (1995) *Hoppe-Seyler's Z. Biol. Chem.*, **376**, 195–198.
7 Kozak,M. (1987) *Nucleic Acids Res.*, **15**, 8125–8148.

8 Stull,R.A., Taylor,L.A. and Szoka,F.C.J. (1992) *Nucleic Acids Res.*, **20**, 3501–3508.
9 Laptev,A.V., Zichun,L., Colige,A. and Prockop,D.J. (1994) *Biochemistry*, **33**, 11033–11039.
10 Ehresmann,C., Baudin,F., Mougel,M., Romby,P., Ebel,J.-P. and Ehresmann,B. (1987) *Nucleic Acids Res.*, **15**, 9109–9128.
11 Knapp,G. (1989) In Dahlberg,D.E. and Abelson,J.N. (eds), *Methods in Enzymology—RNA Processing:* Part A, *General Methods.* Academic Press, New York, NY, pp. 180 and 192–211.
12 Latham,J.A. and Cech,T.R. (1989) *Science*, **245**, 276–282.
13 Han,H., Schepartz,A., Pellegrini,M. and Dervan,P.B. (1994) *Biochemistry*, **33**, 9831–9844.
14 Trevorrow,K., Valet,G., Tapiero,H., Savaraj,N. and Lampidis,T. (1991) *J. Cell. Pharmacol.*, **2**, 217.
15 Morvan,F., Porumb,H., Degols,G., Lefebvre,L., Pompon,A., Sproat,B.S., Rayner,B., Malvy,C., Lebleu,B. and Imbach,J.-L. (1993) *J. Med. Chem.*, **36**, 280–287.
16 Monia,B.P., Lesnik,E.A., Gonzalez,C., Lima,W.F., McGee,D., Guinosso,C.J., Kawasaki,A.M., Cook,P.D. and Freier,S.M. (1993) *J. Biol. Chem.*, **268**, 14514–14522.
17 Inoue,H., Hayase,Y., Iwai,S. and Ohtsuka,E. (1987) *FEBS Lett.*, **215**, 327–330.
18 Hayase,Y., Inoue,H. and Ohtsuka,E. (1990) *Biochemistry*, **29**, 8793–8797.
19 Uchiyama,Y., Miura,Y., Inoue,H., Ohtsuka,E., Ueno,Y., Ikehara,M. and Iwai,S. (1994) *J. Mol. Biol.*, **243**, 782–791.
20 Ma,W.P., Hamilton,S.E., Stowell,J.G., Byrn,S.R. and Davisson,V.J. (1994) *Bioorg. Med. Chem.*, **2**, 169–179.
21 Richert,N.D., Aldwin,L., Nitecki,D., Gottesman,M.M. and Pastan,I. (1988) *Biochemistry*, **27**, 7607–7613.
22 Roninson,I.B. (1991) *Molecular and Cellular Biology of Multidrug Resistance in Tumor Cells.* Plenum Press, New York, NY.
23 Efferth,T., Lohrke,H. and Volm,M. (1989) *AntiCancer Res.*, **9**, 1633–1638.
24 Roller,E., Klumpp,B., Krause,J., Eichelbaum,M. and Schumacher,K. (1993) *Cancer Chemother. Pharmacol.*, **32**, 151–155.
25 Ueda,K., Clark,D.P., Chen,C.J., Roninson,I.B., Gottesman,M.M. and Pastan,I. (1987) *J. Biol. Chem.*, **262**, 505–508.